Hindawi
Geofluids
Volume 2022, Article ID 8130555, 15 pages
https://doi.org/10.1155/2022/8130555

Research Article

The Investigation of Strata Control for Ultrasoft Coal Seam Mining

Chuanqi Zhu, Lei Wang, and Shaobo Li

State Key Laboratory of Mining Response and Disaster Prevention and Control in Deep Coal Mines, Anhui University of Science and Technology, Huainan 232001, China

Correspondence should be addressed to Chuanqi Zhu; cqzhu@aust.edu.cn

Received 31 May 2021; Revised 21 July 2021; Accepted 25 February 2022; Published 16 April 2022

Academic Editor: Zhijie Wen

Strata control of ultrasoft coal seam has been a critical problem for mining and geotechnical engineers in years. In this paper, the No. 66207 longwall panel at Xinzhuangzi coal mine, Anhui, China, was used as an example for study. A systematic approach using laboratory testing, numerical simulation, and field validation was implemented to investigate the influences of roadway layout and presplit blasting on mechanical properties of surrounding rock. Based on the results, an inward-stagger roadway layout with presplit blasting on roof was proposed for the regional strata control. The investigation on the relationship between angle of repose of ultrasoft coal and water content showed that the angle of repose first increased then decreased with increasing water content. The peak value was observed at 17.659% water content, suggesting water injection into ultrasoft coal seam can improve the coal mechanical properties and rib stability. The "high resistance, integral beam, two-stage rib+roof support system" was design to replace the traditional equipment, which can support the ultrasoft coal seam. The combination of this system and proposed "difference stepping" mining technique was capable of preventing roof and rib from failure, as well as mitigating the rockfall during moving hydraulic support. Based on the field validation, it was found that the stress concentration coefficient was relatively low during mining process. This was able to effectively manage the mining-induced stress while improving the productivity three times than without the technique. There was also no failure event observed during mining, such that the safety of mine workers was improved significantly.

1. Introduction

The occurrence conditions of Chinese coal resources are very complex, with soft coal seams widely distributed and extremely rich reserves. According to incomplete statistics, 53.3% of Chinese coal mines contains soft coal seams [1]. Huainan and Huaibei in Anhui, China, has significant high quality coal reserves, particularly in No. 7 and No. 8 areas. However, the mine site is under complex geological conditions, including various shapes of folds and densely distributed preexisting fractures, as displayed in Figure 1(a). Coal cut by the shearer is very loose and small, showing high porosity when it is stockpiled, as shown in Figure 1(b). Coal at the longwall face is extremely loose and fractured with low strength and almost zero cohesion, which can be broken by hands. When mining this type of ultrasoft coal seam, the longwall face collapses along with mining. At the same time, coal rib is rarely complete and competent, which in turn leads to roof failure, hydraulic support instability, and falling gangue. These hazardous events are harmful to the mine workers as well as production, especially for coal seams with high inclinations and high mining heights. Therefore, it is critical to investigate the strata control for this type of coal seams to ensure the safety and productivity.

In the study of coal and rock instability model Li et al. [2] established the coal instability risk analysis and prediction model by using the dynamic fuzzy logic method and tested the effectiveness and feasibility of the model. Based on 11224 working face of Panji No. 2 coal mine in Huainan Mining Area, Liu et al. [3] established the mechanical model of coal wall sliding instability and analyzed the characteristics of coal wall instability. Si et al. [4] put forward a new SVM algorithm

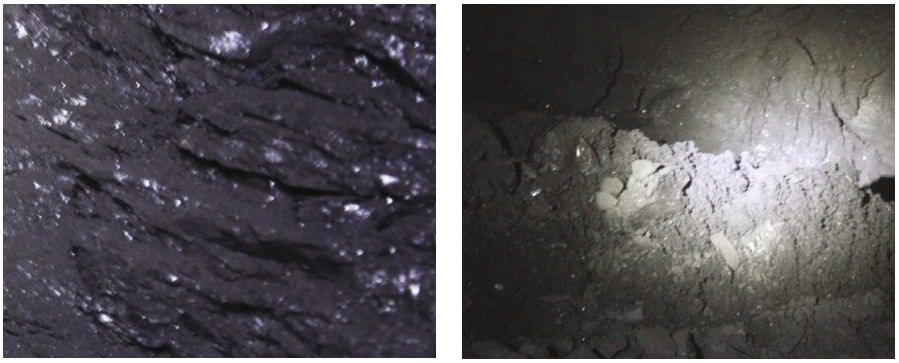

(a) (b)

Figure 1: Geological conditions of coal seam, (a) rib, and (b) loose coal.

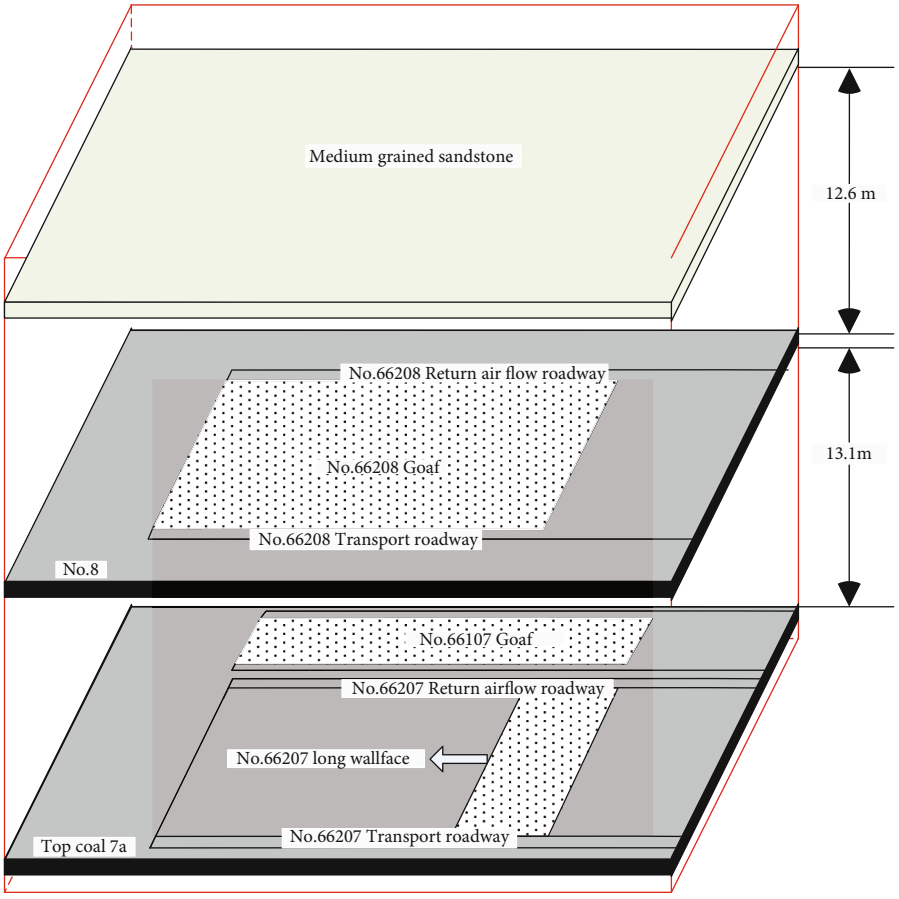

Figure 2: Location of No. 66207 seam.

for coal and rock instability disaster, established the coal and rock instability risk evaluation model, and verified the feasibility and superiority of the model. Li and Zhang [5] established the unloading field effect model of coal wall excavation according to the distribution characteristics of surrounding rock stress field of large mining height working face, analyzed the instability mechanism of coal wall under the action of unloading stress field, and put forward the prevention measures to improve the wall protection force, support initial support force, and coal cohesion. Li et al. [6] established the mechanical model of coal wall sliding instability, derived the analytical expression of the safety factor of each sliding surface, took 8102 working face of wulonghu coal mine as an example, solved the safety factors of different sliding surfaces, and obtained the critical sliding surface position and maximum sliding depth of coal wall. Yuan et al. [7] proposed a constitutive model for "wedge" sliding of coal rib and investigated the influential factors of rib stability. Yin et al. [8] developed constitutive models which describe the rib instability along slab tracing and weak inclusion. Thereby, a rib failure prediction tool for LTCC using C++ was proposed. Guo et al. [9] studied the interaction among coal wall, support, and roof

Comprehensive bar chart		Mechanical parameters of coal and rockmass								
Columnarsection	Lithology of columnar section	Thickness (m)	Bulk density (KN/m^3)	Elastic modulus (GPa)	Poisson's ratio	Cohesion (MPa)	Angle of internal friction (°)	Bulk modulus (GPa)	Shear modulus (GPa)	Tensile strength (MPa)
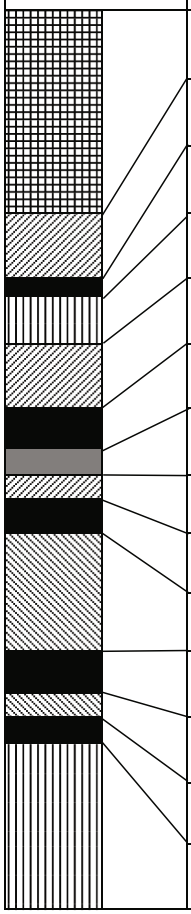	Medium grained sandstone	11.0	28.20	25.33	0.23	3.35	39	9.96	8.62	1.59
	Sandy mudstone	3.8	26.65	23.21	0.17	2.61	41	11.72	9.92	1.21
	No.9	0.8	27.00	24.02	0.20	2.78	40	13.33	10.00	1.35
	Siltstone	3.0	26.65	23.21	0.17	2.61	41	11.72	9.92	1.21
	Sandy mudstone	4.5	24.61	8.81	0.26	1.2	30	6.08	3.47	0.61
	No.8	1.9	27.00	24.02	0.20	2.78	40	13.33	10.00	1.35
	Fine sandstone	1.5	25.49	14.41	0.24	1.78	34	9.23	5.81	0.88
	Sandy mudstone	1.5	24.61	8.81	0.26	1.2	30	6.08	3.47	0.61
	No.7b	1.1	13.7	5.13	0.32	1.25	32	4.72	1.93	0.13
	Mudstone	9.0	24.2	14.31	0.21	1.42	32	7.73	8.63	0.76
	Top coal 7a	2.7	13.7	5.13	0.32	1.25	32	4.72	1.93	0.13
	Mudstone	1.3	24.2	14.31	0.21	1.42	32	7.73	8.63	0.76
	Bottom coal 7a	1.0	13.7	5.13	0.32	1.25	32	4.72	1.93	0.13
	Siltstone	10.0	26.65	23.21	0.17	2.61	41	11.72	9.92	1.21

Figure 3: Mechanical properties of roof and floor.

by analyzing the mechanical model of support surrounding rock under different roof structures and put forward the control measures for the stability of deep hole static pressure pregrouting coal wall.

In the study of instability of surrounding rock, Yuan et al. [10] focused on the development, expansion and penetration of cracks on the coal wall of the working face in soft coal seam, and finally put forward the water injection prevention technology. In order to effectively control the surrounding rock instability accident of short wall coal seam with large mining height in soft thick coal seam, Yuan et al. [11] developed a drilling shearer and drilling mining technology and successfully applied them in 1305 working face of Zhaozhuang coal mine. Behera et al. [12] analyzed the key factors affecting the stability of coal and rock in Godavari Valley coalfield working face and put forward the damage criterion for quantifying the stability of coal wall in working face. Li G. S. et al. [13] studied the failure characteristics of coal wall spalling in thick coal seam with gangue, analyzed the morphology of coal wall spalling in different gangue positions, and found that coal seam with gangue is more prone to spalling at the gangue position. Yao et al. [14] comprehensively studied the supporting stress distribution in front of the working face under different mining dip angles and determined the main failure forms and positions of coal wall. Based on the propagation law of stress wave, Lu et al. [15] took the coal wall of deep working face as the research object and analyzed the dynamic damage and failure characteristics of coal wall from the perspective of dynamics. Tian et al. [16] analyzed the failure mechanism of rib under high mining height using the data from No. 4 coal seam at Longquan coal mine. Based on the investigation, the researchers obtained the relationship between rib failure and hydraulic support working resistance and determined the appropriate mining method which can prevent rib failure. Wang [17] studied the ultrasoft coal seam ribs and proposed a number of control technique, including Longwall Top Coal Caving (LTCC), improving hydraulic support resistance, water injection into coal seam, increasing mining rate, and reducing mining height. Based on the No.

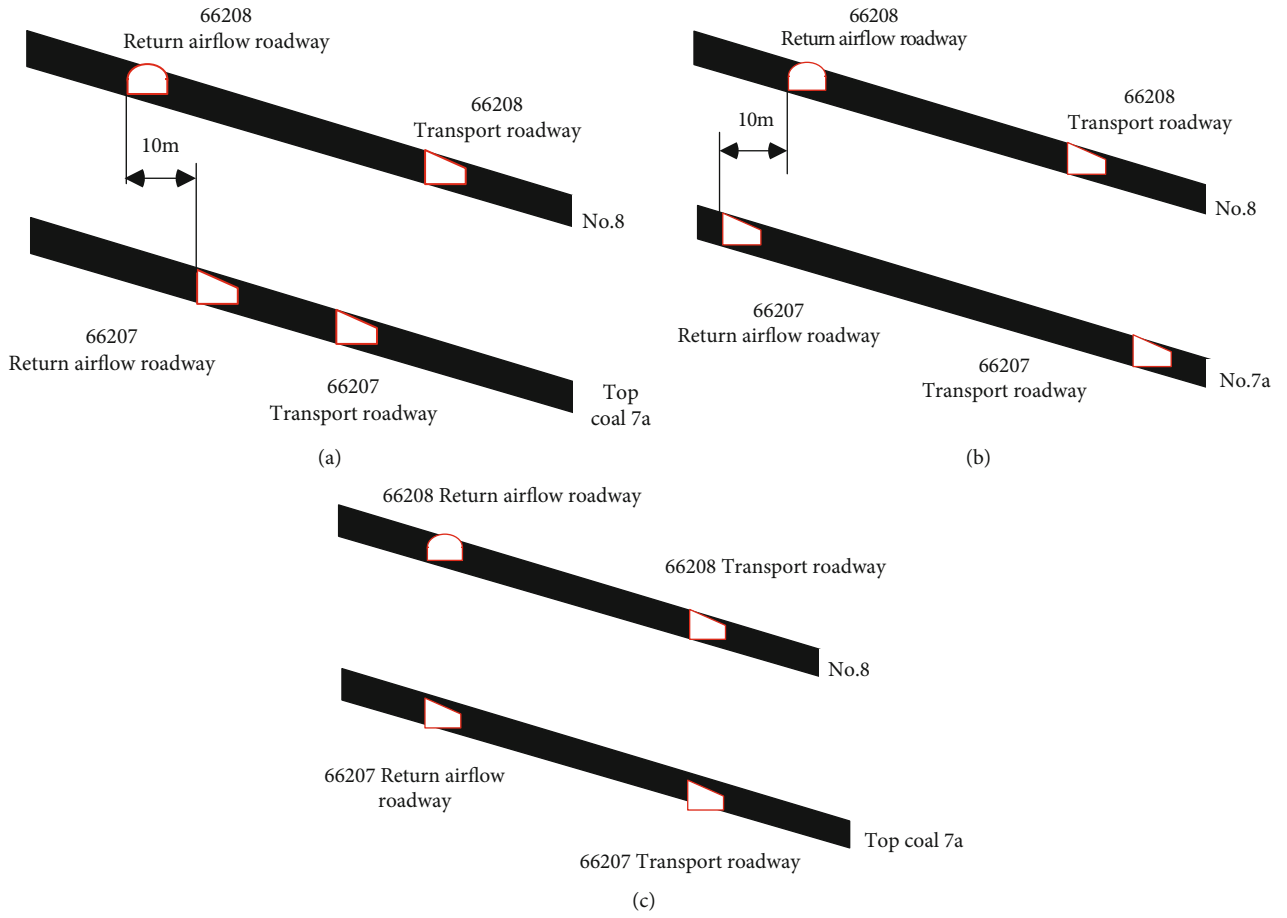

Figure 4: Different layouts for roadway. (a) 10 m inward-stagger layout, (b) 10 m outward-stagger layout, and (c) overlapping layout.

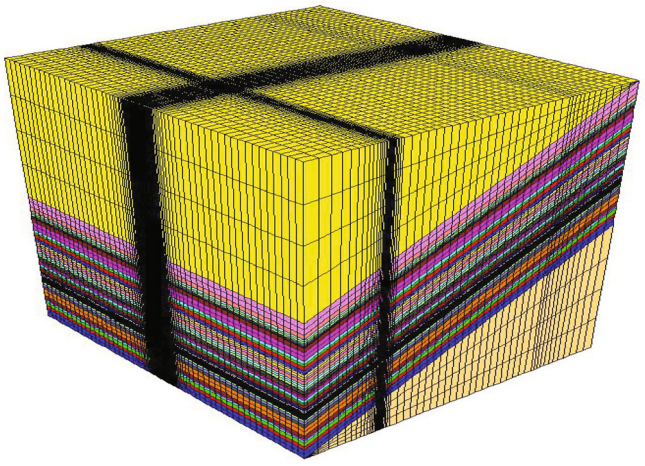

Figure 5: 3D simulation network.

1123 coal seam in Changzishan coal mine, Wu et al. [18] investigated the rib failure mechanism and characteristics and high risk areas under high inclination LTCC longwall face. Subsequently, the researchers suggested a comprehensive controlling technique. Huang and Liu [19] simulated the rib failure process under different mining heights for shallow coal seam via UDEC. Based on the results, the study suggested a series of control techniques, including improving roof support and increasing mining rate and rib support. Fang et al. [20] determined the supporting plan and parameters for Wuyang coal mine rib failure based on coal rib status and root cause as well investigated the stress distribution. Pang et al. [21] divided the rib failure process into two steps: (i) rib failure occurrence and (ii) rib instability and conducted sensitivity analysis on various parameters. Zhang and Wu [22] investigated the rib failure characteristics, influential parameters, and mechanisms under high inclination and high mining heights using monitoring data, numerical simulation, and theoretical analysis. Wang et al. [23] used similar approaches to investigate the stress and displacement distributions in ribs under various mining heights and found that the likelihood of rib failure increases with the increasing mining height. Yang et al. [24] discussed the rib failure mechanism of thick coal seam based on the Ruilong coal mine and conducted sensitivity analysis of controlling factors. According to the analysis, Yang et al. suggested that reducing mining height, improving support, and rib grouting are the effective measures of rib failure. Guo et al. [25] analyzed the relationship between rib failure and immediate roof failure when mining upwards. The paper subsequently defined the required hydraulic support and columns inclination angle. Xia et al. [26] investigated the relationship between longwall mining height and rib instability in LTCC

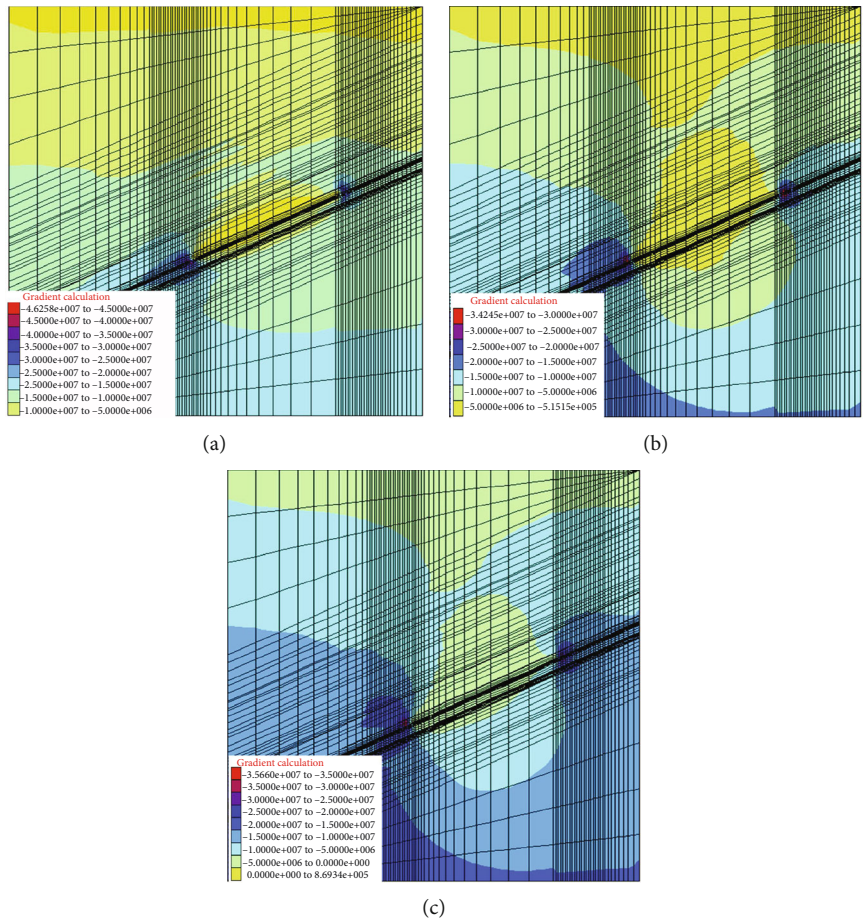

Figure 6: Cloud map of stress distribution along the inclined direction of coal seam, (a) inward-stagger, (b) outward-stagger, and (c) overlapping.

using FLAC3D. Results showed that increasing longwall mining height leads to rib deformation and fracture, which then results to rib failure and roof failure. Yang et al. [27] studied the rib stability of longwall face with gangue using laboratory investigation and theoretical analysis. Li et al. [28] analyzed the compressive shearing, sliding, splitting, or horizontal arching failures of coal rib based on Hetangou coal mine. Based on the analysis, Li et al. suggested to change the stress distribution in order to ensure rib stability. Zhang [29] analyzed the influences of stress distribution and rib characteristics on rib instability and proposed associated control techniques.

However, majority of previous studies focused on the instability of surrounding rock under high mining heights, whereas there is lack of attention for ultrasoft coal seams. Hence, this paper will investigate the instability of surrounding rock of ultrasoft coal seam based on the data collected from No. 66207 longwall face at Xinzhuangzi coal mine and propose the key equipment and techniques for strata control.

2. Engineering Background

2.1. Mechanical Properties of Coal. No. 7 mining area in Huainan contains dry and fractured coal (1.336% water content) with particle size less than 10 mm. There are 47.157% of particle size less than 2.5 mm, and the rock strength is extremely low, and the Platts coefficient is only 0.382.

2.2. Coal Reserve and Mining Conditions. No. 66207 longwall face has the maximum and minimum elevations of -721 m and -793 m. The coal seam thickness is between 1.7 and 4.8 m, with average thickness of 2.7 m. The inclination angle is 27°-34°with average angle of 30°. No. 7 seam has two subseams (No. 7 top and No. 7 bottom), and some parts converge into one seam. No. 7 top thickness is between 1 and 3.2 m, and the seam has average thickness of 2.7 m; whereas, No. 7 top thickness is between 0.7 and 1.7 m and the seam has an average thickness of 1 m. The interburden is between 0 and 1.7 m, with average thickness of 1.3 m.

Mining has completed at the last stage of No. 66107 and No. 66208 above, whereas mining at B6 seam beneath has not yet been commenced. Figure 2 shows the location of No. 66207 seam. This longwall face is between the F5-3 and F6 fault zones, where the north of longwall is close to F5-3. There is large change in the stratum with folds. The in situ stress is concentrated at the longwall face, and the surrounding geology is complex with noticeable faults.

2.3. Mechanical Properties of Roof and Floor. Based on the laboratory and field tests [30], the mechanical properties of

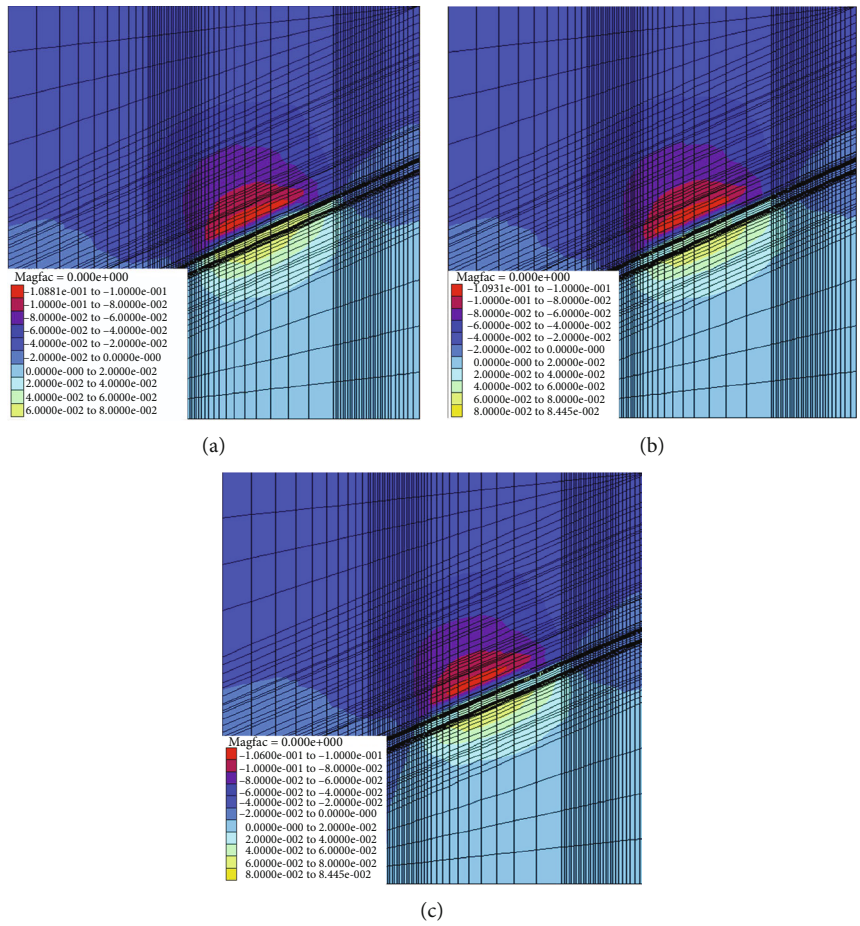

Figure 7: Cloud map of displacement distribution along the inclined direction of coal seam. (a) Inward-stagger, (b) outward-stagger, and (c) overlapping.

roof and floor were obtained, as shown in Figure 3. The immediate roof consists of 2-12 m mudstone, with average thickness of 9 m. The immediate floor is 6-19 m siltstone, with average thickness of 10 m.

Coal at No. 66207 is loose and fractures, which cannot self-sustain under high stress conditions. The distance between the seam and above seam is only 13.3 m. The residual pillars in above coal work (No. 8) caused stress concentration which will influence the safety of No. 66207. There is also medium-grained sandstone 12.6 m above the No. 8 with 11 m thickness. This strong rock layer will result in stress concentration at No. 66207 during mining, which can lead to macroscale instability.

3. Strata Control of Ultrasoft Coal Seam Mining

3.1. Preregional Control Technique via Mining Stress Reduction. FLAC3D was used to analyze the influence of various roadway layouts (inward- and outward- stagger and overlapping) on the stability of surrounding rock. Figure 4 shows the simulation of mechanical properties of surrounding rock under different layouts of No. 66207 longwall [31].

The model has the dimensions of 600 m × 550 m × 523.4 m. The horizontal displacement was constrained on side boundaries, whereas the vertical displacement was constrained on bottom boundary. Load was applied on the model vertically to simulate the overburden weight, see Figure 5. The mechanical properties of each strata is displayed in Figure 3.

Figures 6–8 show cloud maps of stress and displacement fields and fracture distribution of three layouts at No. 66207 longwall. Based on the figures, it can be seen that at the outward-stagger and overlapping layouts, the vertical stress was more concentrated, at 25 MPa and 20 MPa, respectively. Thereby, the vertical displacement was higher and there was some tensile and shear failures observed in the coal seam. On the other hand, 10 MPa vertical stress was observed in inward-stagger layout with maximum vertical displacement of 2 cm. Rock fracture and vertical stress concentration under this condition were not insignificant.

When the outward-stagger or overlapping layout was implemented, there was high stress concentration appeared at some regions along the dip direction of coal seam. Due to the pressure from longwall face, the deformation of surrounding rock gradually increased. This may lead to the likelihood of instability of surrounding rock. When the inward-stagger

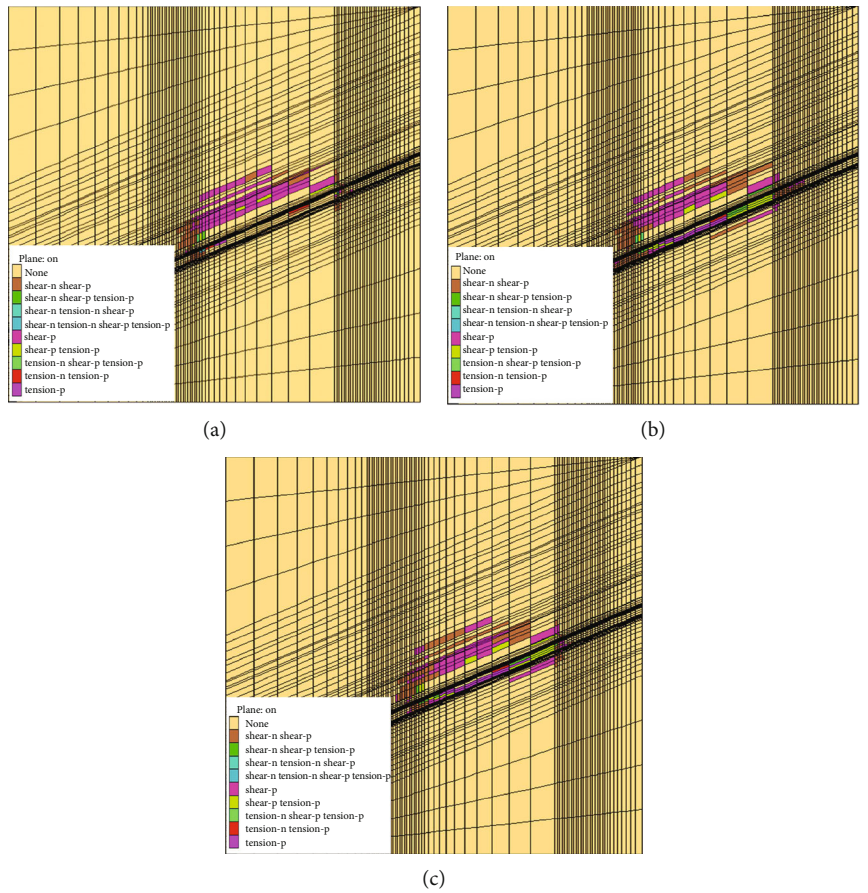

Figure 8: Cloud map of fracture distribution along the inclined direction of coal seam. (a) Inward-stagger, (b) outward-stagger, and (c) overlapping.

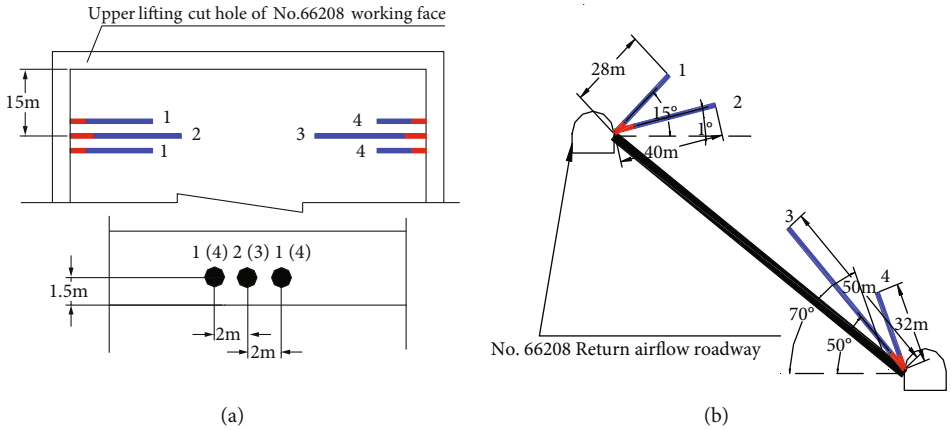

Figure 9: 1st set of blasting hole layout. (a) Plane view and (b) section view.

layout was setup, longwall face and roadway are under the stress relief zone of goaf area. This can effectively reduce the stress concentration while increasing the mining safety.

3.1.1. Stress Redistribution in Roof via Presplit Blasting

(1) Mechanical Properties of Surrounding Rock Prior and after Presplit Blasting. To reduce the stress concentration at the No. 66207 longwall face, the presplit blasting at immediate roof of No. 8 coal seam is considered. The numerical simulation schemes are as follows: The model is 600 m long along the strike, 500 m wide along the slope, and 456.36 m high. The model includes 7# coal, 8# coal, and the roof and floor strata. The average dip angle of the simulated coal seam in the model is 30°, which is consistent with the field.

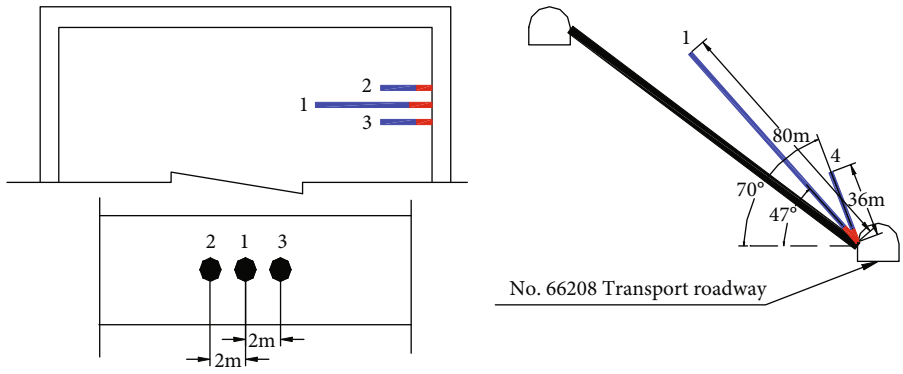

Figure 10: 2nd to 5th set of blasting hole layouts. (a) Plane view and (b) section view.

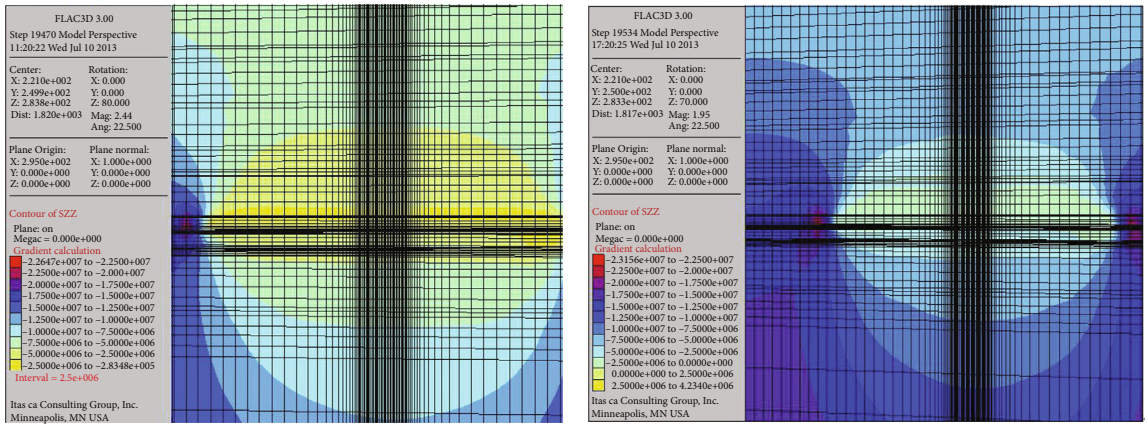

Figure 11: Cloud map of cross-sectional stress distribution 5 m behind along the strike direction of coal seam. (a) Prior to presplit blasting and (b) after presplit blasting.

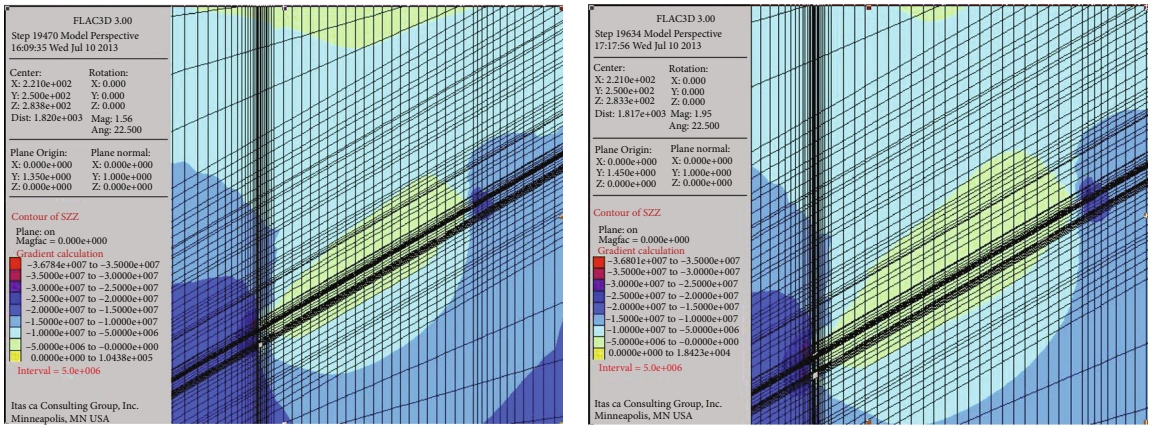

Figure 12: Cloud map of cross-sectional stress distribution 5 m behind along coal seam inclined dip direction. (a) Prior to presplit blasting and (b) after presplit blasting.

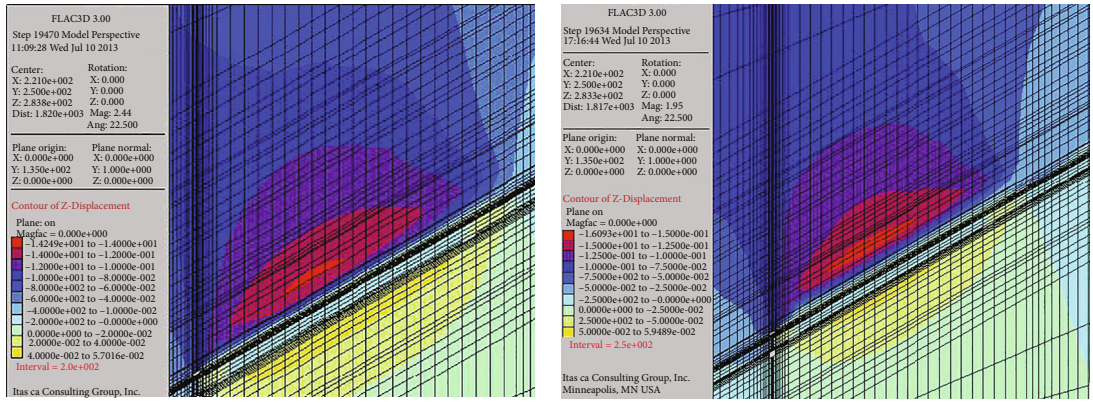

(a) (b)

Figure 13: Cloud map of cross-sectional displacement distribution 5 m behind along the inclined direction of coal seam. (a) Prior to presplit blasting and (b) after presplit blasting.

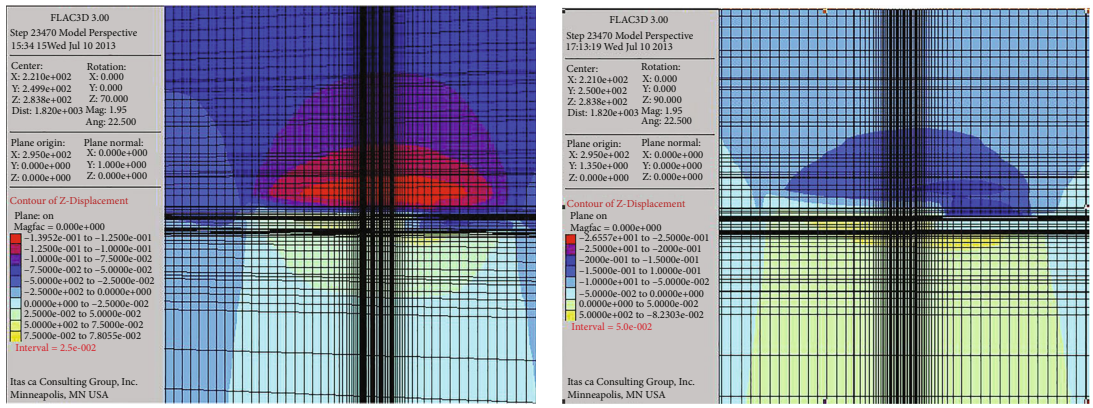

(a) (b)

Figure 14: Cloud map of cross-sectional displacement distribution 5 m behind along the strike direction of coal seam. (a) Prior to presplit blasting and (b) after presplit blasting.

The strength parameters of coal and rock mass around the blast hole are weakened to simulate presplitting blasting.

In deep hole presplit blasting parameters, when the deep hole blasting is used at the longwall face, the designed blasting height is 23 m. This enables the fracture development in the critical layer. There are 5 series of blasting planned, at 30 m interval. The 1st series uses simultaneous blasting at main gates and tail gates, in which the hole locations are shown in Figure 9. Figure 10 shows the hole locations for 2nd to 5th series.

Figures 11–16 provide the simulation results of stress, displacement, and rock fracture when the longwall face is at 70 m. According to the figures, it can be seen that the maximum vertical stress was 50–85 MPa from 90 m to 0 m ahead of the longwall face without presplit blasting, whereas the maximum vertical stress was 25–50 MPa from 90 m to 0 m ahead of the longwall face with presplit blasting.

Prior to presplit blasting, it is important to confirm that the vertical displacement should be within 250 mm from 10 m ahead of the face and majority of the roof is moving. After presplit blasting is implemented, the vertical displacement should be less than 50 mm in the same area.

The fracture was developed at 14 m above No. 8 coal seam prior to the implementation of deep hole presplit blasting, there would be a likelihood of roof rupture and result in increasing load from the roof weighting. This was unfavorable to the stability of surrounding rock. After the blasting, the fracture height above the coal seam was not further developed.

Prior the presplit blasting, the first weighting interval was 67.8 m and the periodic weighting interval was 41.3 m. After blasting, the first and periodic weighting intervals were 24.6 m and 21.9 m, respectively. The interval and time of weighting were reduced after presplit blasting. This led to reduction in load and frequency of weighting, which in turn result in less dynamic load and less pressure ahead of the longwall face. Presplit blasting disturbed the integrity of the strong roof and evenly distributed the stress while reducing the weighting magnitude, which is beneficial to the stability of No. 66207.

3.2. Reinforcement of Strata with Water Injection

3.2.1. The Influence of Water Content on Coal Stability. Firstly, granular coal with particle size in the range of 0.1-

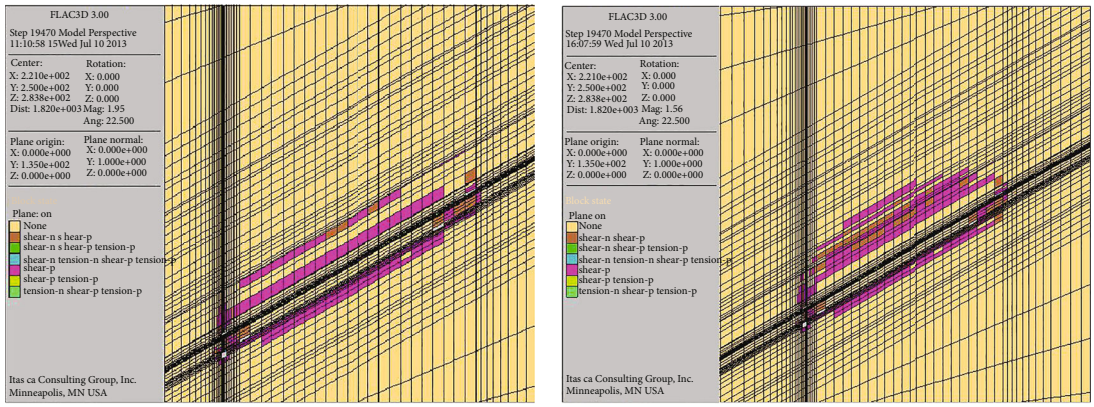

(a) (b)

Figure 15: Cloud map of cross-sectional fracture distribution 5 m behind along the inclined direction of coal seam. (a) Prior to presplit blasting and (b) after presplit blasting.

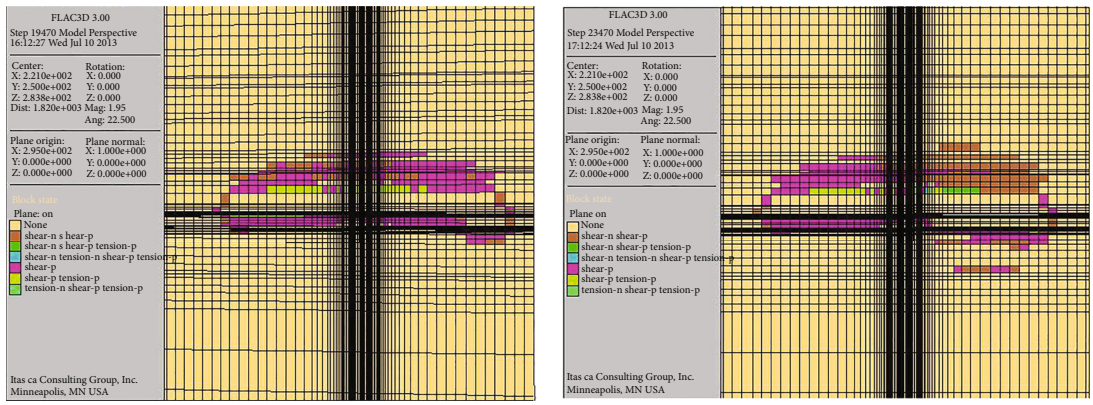

(a) (b)

Figure 16: Cloud map of cross-sectional fracture distribution 5 m behind along the strike direction of coal seam. (a) Prior to presplit blasting and (b) after presplit blasting.

0.25 mm was screened from the dried crushed coal. Then, eight wet pulverized coal samples with different moisture content were made of more than 1000 g granular coal and different qualities of pure water. There are three samples of each moisture content. Finally, the repose angle of wet pulverized coal samples was measured by stacking method, and each group of tests was carried out three times.

To investigate the influence of water content on coal stability, a series of tests on angle of repose of ultrasoft coal were conducted (see Figure 17). Figure 18 shows the relationship between angle of repose of coal and water content. Based on the figure, it can be seen that as the water content increases, the angle of repose decreases. The responding water content with regard to the peak value is 17.659%. This means water injection into the ultrasoft coal seam can change its mechanical properties and improve its stability.

3.2.2. Longwall Water Injection Technique and Parameters. In the field, water injection is conducted at the ribs of both roadways with deep holes (see Figure 19). The step-by-step procedures of deep hole (hole length > 80 m) is that water is injected at both roadways. The distance between hole at the tailgate and the roof should be below 0.8 m, and the hole should be at the center of the coal along the main gate. Water should be injected intermittently all day from 100 m to 20 m ahead of the longwall face. Shallow hole (hole length < 8 m) water injection should have holes 0.5–1 m from the roof. The holes should be drilled perpendicular of subperpendicular to the coal seam side of rib. Sealer should be place 1.5 m into the hole, and the water pressure should be around 2 MPa. Water injection takes place twice a day with at least three hours per injection.

3.3. Rigid-Flexi Active Support Technology. Surrounding rock at ultrasoft coal seam undergoes plastic deformation due to high stress concentration and continuous mining [32]. This would lead to instability of the longwall face and cause injury. To overcome the complex geological condition at No. 66207, ZZ7200/22/45 hydraulic support is selected, with the resistance force of 8800 kN. This equipment can redistribute stress along the roof while more effectively support rib and roof. The new hydraulic support uses an integral

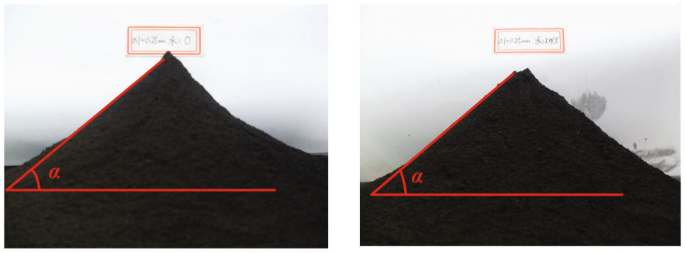

(a) $w = 0.00\%$ (b) $w = 1.01\%$

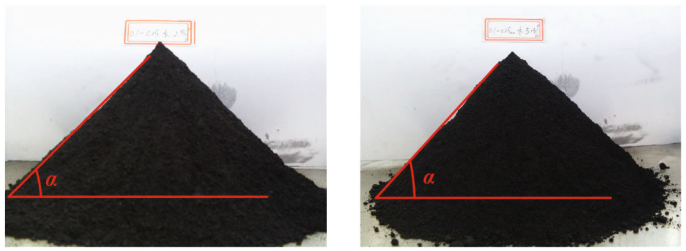

(c) $w = 2.95\%$ (d) $w = 5.13\%$

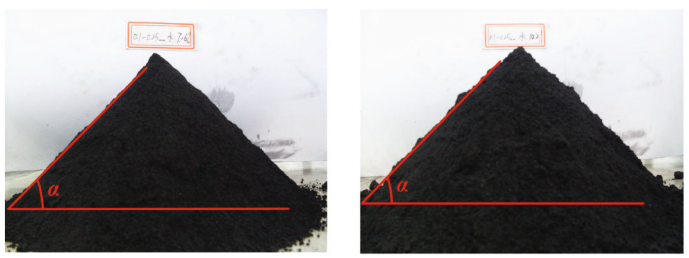

(e) $w = 7.16\%$ (f) $w = 10.20\%$

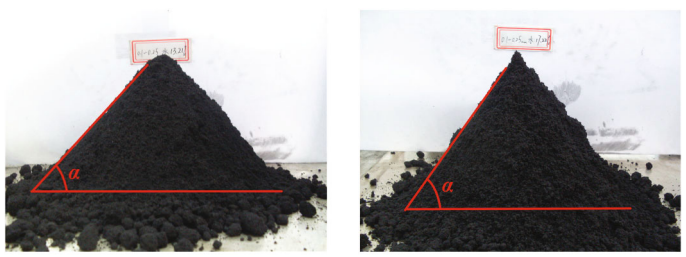

(g) $w = 13.21\%$ (h) $w = 17.22\%$

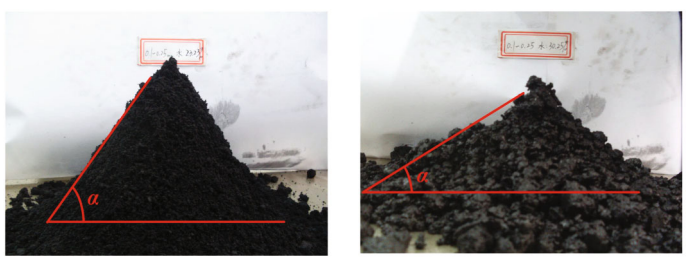

(i) $w = 23.23\%$ (j) $w = 30.25\%$

Figure 17: Accumulation state of coal particles with different water contents.

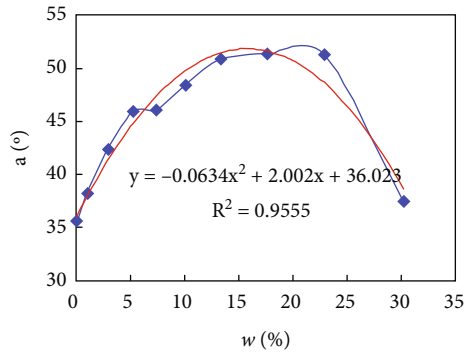

Figure 18: Change of angle of repose of coal with water content.

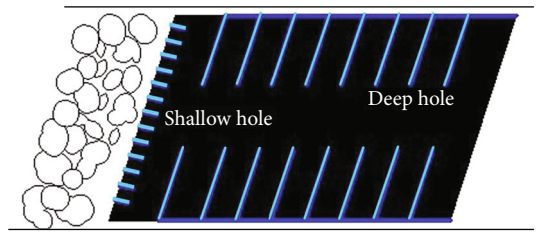

Figure 19: Schematic view of water injection in coal seam.

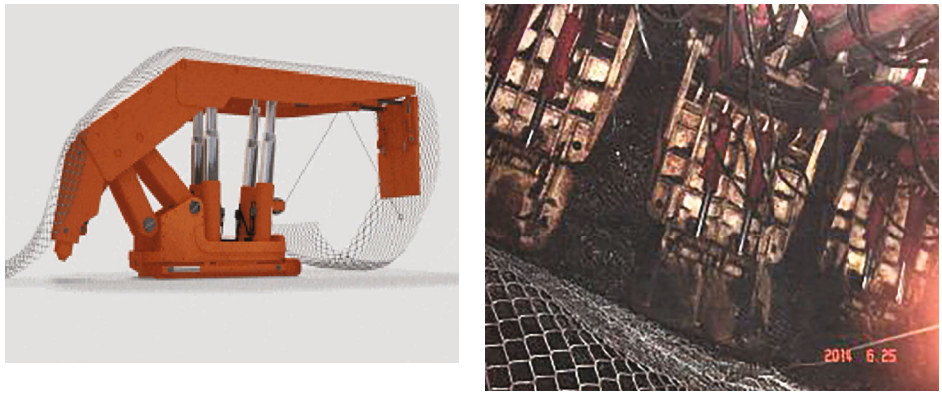

(a) (b)

Figure 20: "Rigid hydraulic support+flexible mesh" supporting system. (a) Support design and (b) support in place.

roof beam structure, which can reduce the disturbance to roof when moving the support. The long flexible beam and two-stage rib support can increase the supporting area and strength to exposed rib and roof, ensuing the integrity of rib and roof.

Figure 20 shows the combination of the hydraulic support and mesh. This approach forms as "high resistance, integral beam, two-stage rib+roof support system," which can effectively prevent the rib and roof from falling and enable the production. The mine operators can be protected in a safety roadway, and the surrounding rock can be hold stable.

3.4. "Difference Stepping" Mining Technology. As the ultrasoft coal seam is prone to rib instability and the interval between ribs at roadways is longer than that of the longwall face, the traditional "three machine" equal step equipment is not capable of preventing the partial failure. This may lead to large-scale failure of rib and roof and subsequently result in operation suspension. Hence, this study proposed "flexible beam length (1000 mm)>pushing length (800 mm)>cutting depth of shearer drum (600 mm)" method (see Figure 21). Hence, the selected equipment are ZZ7200/22/45 hydraulic support, MG500/1130-WD shearer, and SGZ800/1050 conveyor belt. Long flexible beam length can cover larger roof area when rib fails. Small shearer drum can reduce the rib and roof damage during cutting and enhance the integrity and stability of the roof and rib. Thereby, the combination between shallow cutting and long flexible beam can prevent drum from damaging the mesh.

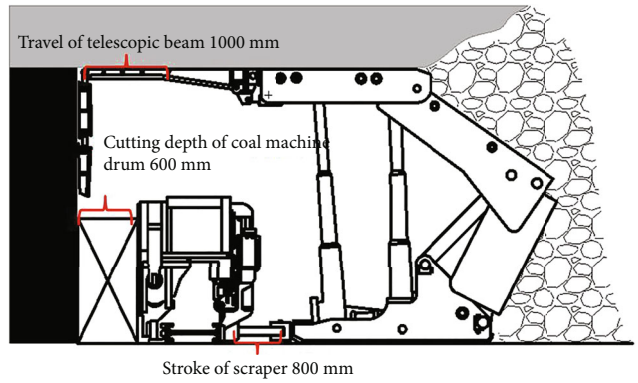

Figure 21: "Difference stepping" three machineries.

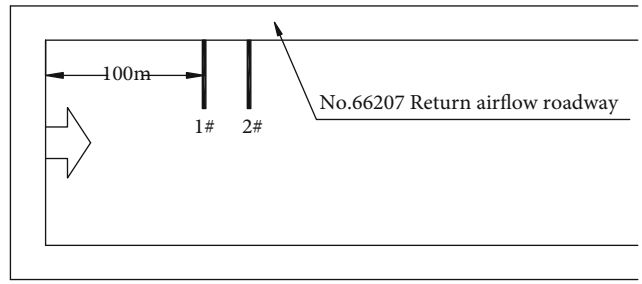

Figure 22: Stress measurement borehole location.

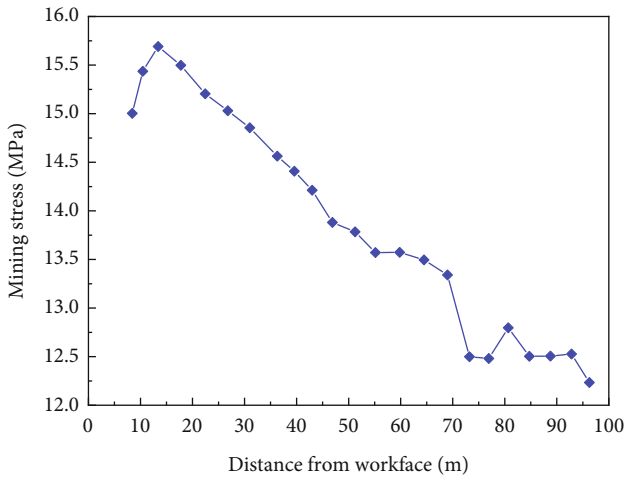

Figure 23: Stress distribution in the coal seam.

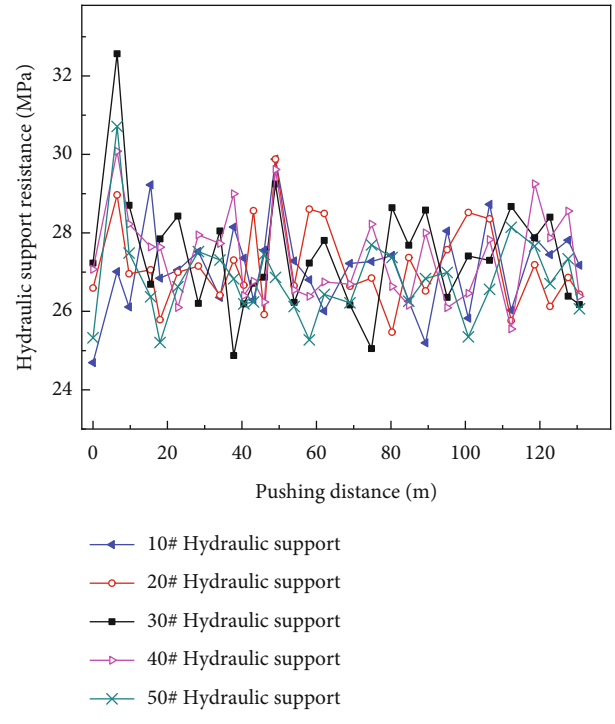

Figure 24: The relationship between hydraulic support resistance and pushing distance.

Pushing support column distance is greater than the drum cutting depth can increase the moving interval and better control the roof stability.

4. Engineering Applications

The stress distribution at No. 66207 longwall face was monitored to examine the effectiveness of proposed strata control technique. Two stress measurements were conducted using KSE-II-1 borehole stress measurement tool at 100 m from the tailgate. The measurement depth and interval were 10 m and 3 m, respectively (see Figure 22).

Figure 23 shows the stress distribution in the coal seam. It can be seen that as the longwall face approached the stress

measurement location within 70 m, stress gradually increased and reached maximum when the distance is approximately 13.5 m. The magnitude of the maximum stress is 15.65 MPa with a stress concentration coefficient of 1.28. After that, stress gradually diminished. During the mining process, the stress concentration coefficient was relatively low and evenly distributed in the concentration area. The location of peak stress concentration is away from the coal rib, such that the excessive stress acting on the rib can be effectively managed.

Figure 24 shows the relationship between hydraulic support resistance and pushing distance. Based on the figure, it can be found that the stress acting on the hydraulic support is generally 26-28 MPa during mining. The hydraulic support is competent under this circumstance and can hold more pressure if needed. The periodic weighting was not obvious in this longwall panel with evenly distributed stress. The weighting interval is approximately 18-21 m with lower mining stress. There was no large scale weighing observed during the mining process.

By comparing the mining rate of No. 66207 longwall panel with the No. 66107 N panel which did not implement the proposed technique, the productivity of No. 66207 was three times of No. 66107 N. In No. 66207 longwall, the average mining rate is 4.35 m/day, with maximum rate at 7.2 m/day. On the other hand, the average mining rate and maximum rate of No. 66107 N were 1.43 m/day and 1.52 m/day. Thereby, there was less failure events occurred in No. 66207, indicating the proposed strata control technique was effective for ultrasoft coal seam.

5. Conclusion

In this study, a strata control technique was proposed for ultrasoft coal seam and it was examined at No. 7 coal seam in Huainan mining area. The technique comprises of mining stress reduction, rock mechanical properties modification of rock, and stability improvement of surrounding rock. The following conclusions were drawn from this study:

(1) Inward-stagger layout used in No. 66207 longwall panel was able to position the longwall face and main gate below the stress relief area of goaf, such that the mining stress concentration can be reduced. The presplit blasting on No. 8 roof was able to evenly distribute the incoming weighting while reducing the weighting intensity. The first weighting and periodic weighting intervals were 24.6 m and 21.9 m after presplit blasting. This technique can prevent weighting on large areas

(2) The investigation on the relationship between angle of repose of ultrasoft coal and water content showed that the angle of repose first increased then decreased with increasing water content. The peak value was observed at 17.659% water content, indicating water injection into ultrasoft coal seam can improve the coal mechanical properties and rib stability

(3) The "high resistance, integral beam, two-stage rib +roof support system" was design to replace the traditional equipment, which can support the ultrasoft coal seam. The combination of this system and proposed "difference stepping" mining technique was capable of preventing roof and rib from failure, as well as mitigating the rockfall during moving hydraulic support

(4) Once the technique was implemented, the stress concentration coefficient was relatively low during mining process. The stress was evenly distributed among the concentration area, and the peak concentration point was away from the longwall face. This was able to effectively manage the mining-induced stress while improving the productivity three times than without the technique. There was also no failure event observed during mining, such that the safety of mine workers was improved

Data Availability

The experimental results used to support the findings of this study are included within the article.

Conflicts of Interest

The authors declare that they have no conflict of interest.

Acknowledgments

The authors are grateful for the National Natural Science Foundation of China (No. 52004007), the Foundation of Educational Commission of Anhui Province (KJ2019A0130), and the Independent Research Foundation of the State Key Laboratory of Mining Response and Disaster Prevention and Control in Deep Coal Mines (SKLMRDPC19ZZ09).

References

[1] C. Liu, *Study on Mechanism and Controlling of Borehole Collapse in Soft Coal Seam [Ph.D. thesis]*, China University of Mining and Technology, Xuzhou, China, 2014.

[2] W. Li, Y. C. Ye, Q. H. Wang, X. H. Wang, and N.-Y. Hu, "Fuzzy risk prediction of roof fall and rib spalling: based on FFTA–DFCE and risk matrix methods," *Environmental Science and Pollution Research*, vol. 27, no. 8, pp. 8535–8547, 2020.

[3] S. Liu, K. Yang, T. Zhang, and C. A. Tang, "Rib spalling 3D model for soft coal seam faces with large mining Height in protective seam mining: theoretical and numerical analyses," *Geofluids*, vol. 2020, Article ID 8828844, 17 pages, 2020.

[4] L. Si, Z. B. Wang, X. H. Liu, C. Tan, and R. X. Xu, "Assessment of rib spalling hazard degree in mining face based on background subtraction algorithm and support vector machine," *Current Science*, vol. 116, no. 12, pp. 2001–2012, 2019.

[5] L. Li and F. Zhang, "Instability model of a coal wall with large mining height under excavation unloading conditions," *Advances in Civil Engineering*, vol. 2020, Article ID 8863602, 6 pages, 2020.

[6] C. Li, T. H. Kang, X. P. Li, L. G. Li, X. Y. Zhang, and R. X. Zhang, "Theoretical investigation of the sliding instability and caving depth of coal wall workface based on the bishop strip method," *Advances in Civil Engineering*, vol. 2019, Article ID 3065930, 8 pages, 2019.

[7] Y. Yuan, S. H. Tu, X. T. Ma, L. L. Sui, and Q. S. Bai, "Study on stability and control of coal wall in fully mechanized face with 'three soft' and large mining height," *Journal of Mining and Safety Engineering*, vol. 29, no. 1, pp. 21–25, 2012.

[8] S. F. Yin, F. L. He, and G. G. Cheng, "Study on criterion of rib spalling and safety evaluation system in fully mechanized top coal caving face with large mining height," *Journal of China University of Mining & Technology*, vol. 44, no. 5, pp. 800–807, 2015.

[9] W. B. Guo, C. Y. Liu, G. W. Dong, and W. Y. Lv, "Analytical study to estimate rib spalling extent and support requirements in thick seam mining," *Arabian Journal of Geosciences*, vol. 12, no. 8, pp. 1–12, 2019.

[10] Y. Yuan, S. H. Tu, X. G. Zhang, and A. X. Liu, "Mechanism and control technique of rib spalling disaster in fully-mechanized mining with large mining height in soft coal seam face," *Disaster Advances*, vol. 6, no. 3, pp. 92–98, 2013.

[11] Y. Yuan, C. Zhu, H. M. Wei, C. F. Yuan, and Z. S. Chen, "Study on rib spalling control of shortwall drilling mining technology with a large mining height," *Arabian Journal of Geosciences*, vol. 14, no. 3, pp. 1–12, 2021.

[12] B. Behera, A. Yadav, G. S. P. Singh, and S. K. Sharma, "A numerical modeling approach for evaluation of spalling associated face instability in longwall workings under massive sandstone roof," *Engineering Failure Analysis*, vol. 117, article 104927, 2020.

[13] G. S. Li, Z. H. Li, F. Du, and Z. Z. Cao, "Study on the failure characteristics of coal wall spalling in thick coal seam with gangue," *Advances in Civil Engineering*, vol. 2020, Article ID 6668458, 10 pages, 2020.

[14] Q. L. Yao, X. H. Li, B. Y. Sun et al., "Numerical investigation of the effects of coal seam dip angle on coal wall stability," *International Journal of Rock Mechanics and Mining Sciences*, vol. 100, pp. 298–309, 2017.

[15] S. F. Lu, S. F. Liu, Z. J. Wan, J. Y. Cheng, Z. Z. Yang, and P. Shi, "Dynamic damage mechanism of coal wall in deep longwall face," *Advances in Civil Engineering*, vol. 2019, Article ID 3105017, 10 pages, 2019.

[16] Q. Z. Tian, A. R. Zhang, Q. K. Lu, Y. F. Liu, and P. X. Li, "Study on coal wall stability of fully mechanized working face with large mining height in thick coal seam," *Journal of Taiyuan University of Technology*, vol. 43, no. 1, 2012.

[17] J. C. Wang, "Rib spalling and prevention mechanism in extremely soft thick coal seam," *Journal of China Coal Society*, vol. 32, no. 8, pp. 785–788, 2007.

[18] Y. P. Wu, D. Lang, and P. S. Xie, "Rib spalling mechanism and disaster mechanism of fully mechanized caving face in soft coal with large dip angle," *Journal of China Coal Society*, vol. 41, no. 8, pp. 1878–1884, 2016.

[19] Q. X. Huang and J. H. Liu, "Analysis on pillar strip model of coal wall spalling in shallow mining face with large mining height," *Journal of Mining and Safety Engineering*, vol. 32, no. 2, pp. 187–191, 2015.

[20] X. Q. Fang, J. He, and H. C. Li, "Study on the mechanism and prevention of the wall of soft coal fully mechanized caving face," *Journal of China University of Mining & Technology*, vol. 38, no. 5, pp. 640–644, 2009.

[21] Y. H. Pang, G. F. Wang, and H. W. Ren, "Multi factor sensitivity analysis of coal wall spalling in large mining height face," *Journal of Mining and Safety Engineering*, vol. 36, no. 4, pp. 736–745, 2019.

[22] H. Zhang and Y. P. Wu, "Rib spalling mechanism of longwall and high mining height stope in steep seam," *Journal of Mining and Safety Engineering*, vol. 36, no. 2, pp. 331–337, 2019.

[23] H. W. Wang, Y. P. Wu, P. S. Xie, S. H. Luo, K. Z. Liu, and M. F. Liu, "Mining thickness effect of coal wall stability in longwall and large mining height working face of large inclined seam," *Journal of Mining and Safety Engineering*, vol. 35, no. 1, pp. 64–70, 2018.

[24] S. L. Yang, D. Z. Kong, J. H. Yang, and H. Meng, "Coal wall stability and grouting reinforcement technology in fully mechanized top coal caving mining," *Journal of Mining and Safety Engineering*, vol. 32, no. 5, pp. 827–839, 2015.

[25] W. B. Guo, Y. Lu, F. C. Huang, C. Y. Liu, M. S. Pei, and Y. S. Du, "Study on the stability and control of coal and rock at the end face of fully mechanized top-coal caving face in upward mining," *Journal of Mining and Safety Engineering*, vol. 31, no. 3, pp. 406–412, 2014.

[26] Y. X. Xia, L. J. Kang, and Q. X. Qi, "Influence of coal cutting height on stability of coal wall in fully mechanized caving face with large mining height," *Coal Science and Technology*, vol. 36, no. 12, 2008.

[27] J. X. Yang, C. Y. Liu, F. F. Wu, and Y. Yang, "The research on the coal wall stability mechanism in larger height coal seam with a stratum of gangue," *Journal of Mining and Safety Engineering*, vol. 30, no. 6, pp. 856–862, 2013.

[28] J. G. Li, Q. Z. Tian, and S. S. Yang, "Coal wall spalling mechanism and control in fully mechanized coal caving mining face in Hetangou mine," *Coal Science and Technology*, vol. 35, no. 12, pp. 73–75, 2003.

[29] X. H. Zhang, *Study on Mechanism Characteristics and Application of Fully Mechanized Top Coal Caving Mining with Great Mining Height in Very Thick Coal Seam, [Ph.D. thesis]*, AnHui University of Science and Technology, Huainan, China, 2012.

[30] M. Gao, J. Xie, Y. Gao et al., "Mechanical behavior of coal under different mining rates: a case study from laboratory experiments to field testing," *International Journal of Mining Science and Technology*, vol. 31, no. 5, pp. 825–841, 2021.

[31] Y. Q. Xu, *Coal Mining*, China University of Mining and Technology Press, 2009.

[32] X. Wang, Z. J. Wen, Y. Jiang, and H. Huang, "Experimental study on mechanical and acoustic emission characteristics of rock-like material under non-uniformly distributed loads," *Rock Mechanics and Rock Engineering*, vol. 51, no. 3, pp. 729–745, 2018.